Advanced perturbation technique for digital backward propagation in WDM systems

Lian Xiang,[1,2] Paul Harper,[2] and Xiaoping Zhang[1,*]

[1]*School of Information Science and Engineering, Lanzhou University, Lanzhou, Gansu 73000, China*
[2]*Aston Institute of Photonic Technologies, Aston University, Birmingham B4 7ET, UK*
[*]*zxp@lzu.edu.cn*

Abstract: An improved digital backward propagation (DBP) is proposed to compensate inter-nonlinear effects and dispersion jointly in WDM systems based on an advanced perturbation technique (APT). A non-iterative weighted concept is presented to replace the iterative in analytical recursion expression, which can dramatically simplify the complexity and improve accuracy compared to the traditional perturbation technique (TPT). Furthermore, an analytical recursion expression of the output after backward propagation is obtained initially. Numerical simulations are executed for various parameters of the transmission system. The results indicate that the advanced perturbation technique will relax the step size requirements and reduce the oversampling factor when launch power is higher than -2 *dBm*. We estimate this technique will reduce computational complexity by a factor of around seven with respect to the conventional DBP.

References and links

1. E. Ip and J. M. Kahn, "Nonlinear impairment compensation using backpropagation," in *Optical Fibre, New Developments* (In-Tech, to be published).
2. P. P. Mitra and J. B. Stark, "Nonlinear limits to the information capacity of optical fibre communications," Nature **411**(6841), 1027–1030 (2001).
3. K. S. Turitsyn, S. A. Derevyanko, I. V. Yurkevich, and S. K. Turitsyn, "Information capacity of optical fiber channels with zero average dispersion," Phys. Rev. Lett. **91**(20), 203901 (2003).
4. T. Pfau, S. Hoffmann, O. Adamczyk, R. Peveling, V. Herath, M. Porrmann, and R. Noé, "Coherent optical communication: towards realtime systems at 40 Gbit/s and beyond," Opt. Express **16**(2), 866–872 (2008).
5. E. Ip, A. P. Lau, D. J. F. Barros, and J. M. Kahn, "Coherent Detection in optical fiber systems," Opt. Express **16**(2), 753–791 (2008).
6. L. B. Du and A. J. Lowery, "Improved single channel backpropagation for intra-channel fiber nonlinearity compensation in long-haul optical communication systems," Opt. Express **18**(16), 17075–17088 (2010).
7. R. Waegemans, S. Herbst, L. Holbein, P. Watts, P. Bayvel, C. Fürst, and R. I. Killey, "10.7 Gb/s electronic predistortion transmitter using commercial FPGAs and D/A converters implementing real-time DSP for chromatic dispersion and SPM compensation," Opt. Express **17**(10), 8630–8640 (2009).
8. S. J. Savory, "Digital filters for coherent optical receivers," Opt. Express **16**(2), 804–817 (2008).
9. R. Asif, C. Y. Lin, and B. Schmauss, *Digital Backward Propagation: A Technique to Compensate Fiber Dispersion and Nonlinear Impairments* (InTech-Book Publisher 2011).
10. E. Mateo, L. Zhu, and G. Li, "Impact of XPM and FWM on the digital implementation of impairment compensation for WDM transmission using backward propagation," Opt. Express **16**(20), 16124–16137 (2008).
11. E. F. Mateo and G. Li, "Compensation of interchannel nonlinearities using enhanced coupled equations for digital backward propagation," Appl. Opt. **48**(25), F6–F10 (2009).
12. X. Li, X. Chen, G. Goldfarb, E. Mateo, I. Kim, F. Yaman, and G. Li, "Electronic post-compensation of WDM transmission impairments using coherent detection and digital signal processing," Opt. Express **16**(2), 880–888 (2008).
13. E. Ip, "Nonlinear compensation using backpropagation for polarization-multiplexed Transmission," J. Lightwave Technol. **28**(6), 939–951 (2010).
14. D. S. Millar, S. Makovejs, C. Behrens, S. Hellerbrand, R. I. Killey, P. Bayvel, and S. J. Savory, "Mitigation of fiber nonlinearity using a digital coherent receiver," IEEE J. Sel. Top. Quantum Electron. **16**(5), 1217–1226 (2010).

15. R. Asif, C. Y. Lin, M. Holtmannspoetter, and B. Schmauss, "Optimized digital backward propagation for phase modulated signals in mixed-optical fiber transmission link," Opt. Express **18**(22), 22796–22807 (2010).
16. D. Rafique and A. D. Ellis, "Impact of signal-ASE four-wave mixing on the effectiveness of digital back-propagation in 112 Gb/s PM-QPSK systems," Opt. Express **19**(4), 3449–3454 (2011).
17. D. Rafique, J. Zhao, and A. D. Ellis, "Digital back-propagation for spectrally efficient WDM 112 Gbit/s PM m-ary QAM transmission," Opt. Express **19**(6), 5219–5224 (2011).
18. G. Goldfarb, M. G. Taylor, and G. Li, "Experimental demonstration of Fiber Impairment compensation using the split-step finite-impulse-response filtering method," IEEE Photon. Technol. Lett. **20**(22), 1887–1889 (2008).
19. S. J. Savory, G. Gavioli, E. Torrengo, and P. Poggiolini, "Impact of interchannel nonlinearities on a split-step intrachannel nonlinear equalizer," IEEE Photon. Technol. Lett. **22**(10), 673–675 (2010).
20. F. Yaman and G. Li, "Nonlinear impairment compensation for polarization-division multiplexed WDM transmission using digital backward propagation," IEEE Photon. J. **2**(5), 816–832 (2010).
21. B. Schmauss, R. Asif, and C.-Y. Lin, "Recent advances in digital backward propagation algorithm for coherent transmission systems with higher order modulation formats," in Proc. SPIE (2012)
22. L. Lin, Z. Tao, L. Dou, W. Yan, S. Oda, T. Tanimura, T. Hoshida, and J. Rasmussen, "Implementation efficient non-linear equalizer based on correlated digital back-propagation," in Proc. OFC (2011).
23. J. Leibrich and W. Rosenkranz, "Efficient numerical simulation of multichannel WDM transmission systems limited by XPM," IEEE Photon. Technol. Lett. **15**(3), 395–397 (2003).
24. E. F. Mateo, F. Yaman, and G. Li, "Efficient compensation of inter-channel nonlinear effects via digital backward propagation in WDM optical transmission," Opt. Express **18**(14), 15144–15154 (2010).
25. E. F. Mateo, X. Zhou, and G. Li, "Improved digital backward propagation for the compensation of inter-channel nonlinear effects in polarization-multiplexed WDM systems," Opt. Express **19**(2), 570–583 (2011).
26. F. Yaman and G. Li, "Nonlinear impairment compensation for polarization-division multiplexed WDM transmission using digital backward propagation," IEEE Photon. J. **1**(2), 144–152 (2009).
27. E. Ip and J. M. Kahn, "Compensation of dispersion and nonlinear impairments using digital backpropagation," J. Lightwave Technol. **26**(20), 3416–3425 (2008).
28. D. Rafique, M. Mussolin, M. Forzati, J. Mårtensson, M. N. Chugtai, and A. D. Ellis, "Compensation of intra-channel nonlinear fibre impairments using simplified digital back-propagation algorithm," Opt. Express **19**(10), 9453–9460 (2011).
29. T. Yoshida, T. Sugihara, H. Goto, T. Tokura, K. Ishida, and T. Mizuochi, "A study on statistical equalization of intra-channel fiber nonlinearity for digital coherent optical systems," in Proc. ECOC' 11, Tu.3.A. (2011)
30. L. Zhu and G. Li, "Nonlinearity compensation using dispersion-folded digital backward propagation," Opt. Express **20**(13), 14362–14370 (2012).
31. W. Yan, Z. Tao, L. Dou, L. Li, S. Oda, T. Tanimura, T. Hoshida, and J. C. Rasmussen, "Low complexity digital perturbation back-propagation," in Proc. ECOC (2011).
32. T. Hoshida, L. Dou, T. Tanimura, W. Yan, S. Oda, L. Li, H. Nakashima, M. Yan, Z. Tao, and J. C. Rasmussen, "Digital nonlinear compensation techniques for high-speed DWDM transmission systems," in Proc.ECOC (2012).
33. G. P. Agrawal, *Nonlinear Fiber Optics* (Academic Press, 2007).
34. A. O. Korotkevich and P. M. Lushnikov, "Proof-of-concept implementation of the massively parallel algorithm for simulation of dispersion-managed WDM optical fiber systems," Opt. Lett. **36**(10), 1851–1853 (2011).
35. L. Xiang and X. P. Zhang, "The study of information capacity in multispan nonlinear optical fiber communication systems using a developed perturbation technique," J. Lightwave Technol. **29**(3), 260–264 (2011).

1. Introduction

In long-haul, high-speed wavelength-division-multiplexed (WDM) optical fiber system non-constructive effects of fiber nonlinearity can significantly degrade signal quality [1]. Therefore, mitigating or compensating these impairments becomes crucial to increasing capacity for optical communication [2]. Many researches have been reported to investigate nonlinearity effect on fiber capacity and indicated that nonlinearity will degrade the capacity obviously [3]. Recently, due to the fast development of digital coherent receiver technology, digital compensation methods have attracted significant attention to mitigate linear and nonlinear impairment effectively as it's flexible and less costly [4,5]. Many digital compensation techniques for different impairments have been already presented [6–8]. Among these techniques, the digital backward propagation (DBP) method has proved to be quite promising for jointly compensating linear and nonlinear impairments [9]. This method is based on solving the nonlinear Schrödinger equation (NLSE) in the backward direction starting with the received signal as the input and producing the signal at the transmitter as its output [10]. But as the high complexity of the NLSE when fiber loss, dispersion and nonlinearity play a crucial role in WDM systems simultaneously, one of the technically challenging for DBP is solving the NLSE effectively in a trade-off between accuracy and computational load [11]. Xiaoxu proposed a universal post-compensation scheme for fiber

impairments in WDM systems using split-step method (SSM) for DBP [12]. Then, SSM as the typically method for conventional DBP (C-DBP) has been applied in many different systems [13–16] and was demonstrated in experiment as well [17,18]. However, this numerical algorithm required a number of iterative processing steps to achieve acceptable accuracy, which is quite a high computational load, thus making it difficult to implement in real-time [19]. Therefore, based on SSM a number of enhanced methods have been reported [20–22]. According to the method proposed by Liebrich et al. [23], Eduardo F. Mateo et al. derived an advanced SSM for DBP in WDM systems, which consisted in the factorization of the walk-off effect within the nonlinear step, and then applied it to the polarization-multiplexed WDM systems [24,25]. It was estimated in that works that such advanced SSM relaxes the step size requirements resulting in a factor of 4 reductions in computational load. However, the accuracy of these numerical methods mentioned previously can be accepted only when the step size h is set within a thin range to keep a small degree of nonlinear phase-shift [26]. But, as a typical value of h is equal to span length in backward propagation [27], a small nonlinear phase-shift is hardly to maintain along each distance h, so that an unsatisfied accuracy is inevitable especially for a large h. Then some other algorithms distinguished from SSM are proposed for backward propagation [28–30]. Based on perturbation analysis, a version of digital back-propagation was proposed to compensate intra-channel nonlinearity in polarization-division multiplexed WDM systems [31,32]. In their work, the inter-channel nonlinear effects which should be the major part of nonlinear effects in WDM system were neglected, meanwhile, the combined nonlinear distortion caused by Kerr nonlinearity and dispersion was also not considered. Therefore, this result is limited in application to the actual WDM systems.

In this paper, an advanced perturbation technique (APT) is developed and basing on this technique, an improved digital backward propagation (DBP) is proposed to compensate inter-nonlinear effects and dispersion jointly in WDM systems. In this advanced perturbation technique, a non-iterative weighted concept is presented to replace the iterative in the analytical recursion expression, which can dramatically simplify the complexity and improve accuracy compared to the traditional perturbation technique (TPT). Furthermore, an analytical recursion expression of the output after backward propagation is obtained initially, which the inter-channel walk-off effect and the combined nonlinear distortion caused by Kerr nonlinearity and dispersion can be consisted in. Comparing to C-DBP, an expression for the total number of required multiplications per sample per channel is given and a rigorous analysis of the computational cost is carried out. Numerical simulations are performed in the corresponding transmission system with various parameters. Our research indicates that APT is more accurate than C-DBP for nonlinearity compensation when launch power is higher than −2 *dBm* and step size is larger than 20 *km*, especially about 2.4 *dB* benefits than C-DBP at 3 *dBm* with one step per span, which will allow larger step size for equivalent performance. Meanwhile, APT requires a lower sampling rate when launch power is higher than −2 *dBm*. For a transmission system with a weaker nonlinear, the Q-factor of APT appears to be a larger peak value. We estimate that there is a reduction in computational complexity by a factor of around seven.

2. Digital backward propagation for WDM systems using advanced perturbation Technique

In the receiver of a coherent optical system, the optical field of each WDM channel, including both the optical amplitude and phase can be measured. To compensate the transmission impairments, DBP processes the received signals by launching them into a virtual fiber with inverse optical link parameters. In practice, it can be implemented by solving the inverse NLSE. For a single polarization the NLSE in WDM systems for backward-propagation is written as [33]:

$$\frac{\partial E_k}{\partial z} - \frac{i\beta_2}{2}\frac{\partial^2 E_k}{\partial t^2} + \frac{\beta_3}{6}\frac{\partial^3 E_k}{\partial t^3} + i\gamma(|E_k|^2 + 2\sum_{q \neq k}|E_q|^2)E_k = G(z)E_k, \qquad (1)$$

where $E_k(z,t)$ is the envelope of the kth channel field, $k, q = \{1,2,...m\}$, m is the number of channels, β_2, β_3 and γ are the second dispersion, third order dispersion and nonlinear parameter, $G(z) = \frac{\alpha}{2} + [e^{\frac{-\alpha}{2}z_a} - 1]\sum_{n=1}^{N}\delta(z-nz_a)$, α is the absorption coefficient, z_a is the span length, N is the number of spans and nz_a are amplifier locations, distributed amplification can be included in G(z) [34]. This equation describes the backward evolution of optical field of WDM channels where dispersion, SPM and XPM can be compensated. As a long step length is demanded for reducing computational cost, the accuracy of SSM will be decreased simultaneously. Combining the flexibility of SSM and the accuracy of perturbation theory, a developed perturbation technique was proposed [35]. Based on this algorithm, firstly, the whole transmission link should be divided into sections and the length (h) of each section can be set flexibly to achieve acceptable accuracy. Then it is considered that the output of lth section is treated as the input of $(l+1)^{th}$ section. In each section, the NLSE is solved using perturbation theory. Applying Fourier transform $\hat{E}_k(\omega,z)=\mathcal{F}[E_k(t,z)]$ to Eq. (1), the output of lth section can be obtained in the frequency domain as follows:

$$\hat{E}_k^{(l)}(\omega,z) = \exp(\hat{D})[\hat{E}_k^{(l-1)} + i\gamma\int_z^{z+h}\hat{NL}_k^{(l-1)}(\omega,z')dz'], \qquad (2)$$

where $\hat{E}_k^{(l-1)}$ is the output of (l-1) section, $\hat{D}$ is the linear operator in the frequency domain and $\hat{NL}_k^{(l-1)}$ is the nonlinear operator, which are given by:

$$\hat{D} = \int_z^{z+h}[G(z') - \frac{i\beta_2\omega^2}{2} + \frac{i\beta_3\omega^3}{6}]dz', \qquad (3)$$

$$\hat{NL}_k^{(l-1)} = \mathcal{F}[-(|\varphi_k^{(l-1)}|^2 + 2\sum_{q \neq k}|\varphi_q^{(l-1)}|^2)\varphi_k^{(l-1)}]\exp(-\hat{D}), \qquad (4)$$

where $\mathcal{F}[\cdot]$ represents the Fourier Transform and

$$\varphi_k^{(l-1)} = \mathcal{F}^{-1}[\hat{E}_k^{(l-1)}\exp(\hat{D})]. \qquad (5)$$

To properly evaluate the phase shift induced by channel q over channel k, the dispersive walk-off induced by a different group delay has to be tracked. This delay between channels q and k occurs on a length scale given by the walk-off length, $L_{wo} = 1/(|\beta_2|B\Delta\omega_{qk})$ [24], where $\Delta\omega_{qk}$ is the frequency difference and B is the baud-rate. By including the time delay caused by the dispersive walk-off, we rewrite Eq. (4) as follows:

$$\hat{NL}_k^{(l-1)}(\omega,z) = -\mathcal{F}[|\varphi_k^{(l-1)}|^2\varphi_k^{(l-1)}]\exp(-\hat{D}) - \mathcal{F}[2\sum_{q \neq k}|\varphi_q^{(l-1)}|^2]e^{-id_{qk}z\omega} * \mathcal{F}[\varphi_k^{(l-1)}]\exp(-\hat{D}), (6)$$

where $*$ represents the convolution and $d_{qk} = \beta_2(\omega_k - \omega_q)$ is the walk-off parameter between channels k and q. As a nonlinear operator, Eq. (6) includes the time delay caused by the dispersive walk-off. By substituting Eq. (5) and Eq. (6) into Eq. (2), the output of lth section

($\hat{E}_k^{(l)}$) can be derived with $\hat{E}_k^{(l-1)}$. Then treating $\hat{E}_k^{(l)}$ as the input of $(l+1)^{th}$ section, after the same procedure, the output of $(l+1)^{th}$ section can be estimated similarly. In this scenario, when the number of sections in the whole transmission link is M , after some reiteration, the output signal after backward propagation can be obtained as follows:

$$\hat{E}_k^{out}(\omega,z) = \hat{E}_k^{(0)} \exp(M\hat{D}) + i\gamma\{\exp(M\hat{D}) \int_z^{z+h} \hat{NL}_k^{(0)}(\omega,z')dz'$$

$$+ \exp((M-1)\hat{D}) \int_z^{z+h} \hat{NL}_k^{(1)}(\omega,z')dz' + \cdots + \exp(\hat{D}) \int_z^{z+h} \hat{NL}_k^{(M-1)}(\omega,z'))dz'\}, \quad (7)$$

where $\hat{E}_k^{(0)}$ is the received signal which is used as the input of backward propagation. As it is impractical to implement integrals in DSP, an approximation of the integral should be applied to Eq. (7). Usually, $\mathcal{F}[-(|\varphi_k^{(l-1)}|^2 + 2\sum_{q \neq k}|\varphi_q^{(l-1)}|^2)\varphi_k^{(l-1)}]$ is treated as constant during each h in traditional perturbation technique (TPT). Then the integral can be solved analytically. But it does not accord with the actual case and will bring a huge error especially in a large h . Here we use the trapezoidal rule for integral. Although the accuracy of trapezoidal rule will be improved with its grid points increasing, a higher computational load will be required. From the computational perspective, trapezoidal rule with one grid point is applied and a discretized form of Eq. (2) can be given by:

$$\hat{E}_k^{(l)}(\omega,z) = \exp(\hat{D})\{\hat{E}_k^{(l-1)} + i\gamma h[\frac{\hat{NL}_k^{(l-1)}(\omega,z) + \hat{NL}_k^{(l-1)}(\omega,z+h)}{2}]\}. \quad (8)$$

It is necessary to follow an iterative procedure that is initiated by replacing $\hat{NL}_k^{(l-1)}(\omega,z+h)$ by $\hat{NL}_k^{(l-1)}(\omega,z)$, then use Eq. (8) to estimate $\hat{E}_k^{(l-1)}(\omega,z+h)$ which in turn is used to calculate the new value of $\hat{NL}_k^{(l-1)}(\omega,z+h)$. Since iteration is time-consuming, a faster non-iterative weighted concept is used instead and a similar form is given by:

$$\hat{E}_k^{(l)}(\omega,z) = \exp(\hat{D})[\hat{E}_k^{(l-1)} + i\gamma h\, \hat{NL}_k^{(l-1)}(\omega,z+\varepsilon h)], \quad (9)$$

where $\varepsilon \in (0,1)$ is a constant which typically is set to 0.5. In this concept, the integral in Eq. (2) is replaced by $h\, \hat{NL}_k^{(l-1)}(\omega,z+\varepsilon h)$, which can reduce the computational complexity effectively. Meanwhile, the constant ε can be set flexibly in different systems to achieve a satisfied accuracy. In this vein, after rewriting Eq. (7), an analytical recursion expression of the output after backward propagation is obtained as follows:

$$\hat{E}_k^{out}(\omega,z) = \hat{E}_k^{(0)} \exp(M\hat{D}) + i\gamma h[\exp(M\hat{D})\, \hat{NL}_k^{(0)}(\omega,\varepsilon h)$$

$$+ \exp((M-1)\hat{D})\, \hat{NL}_k^{(1)}(\omega,\varepsilon h) + \cdots + \exp(\hat{D})\, \hat{NL}_k^{(M-1)}(\omega,\varepsilon h)]. \quad (10)$$

The schematic for implementation of the develop perturbation technique in the lth section is shown in Fig. 1 where for simplicity, $H_d = \exp[\hat{D}(\omega,h)]$, $H_{d,\varepsilon} = \exp[\hat{D}(\omega,\varepsilon h)]$, $H_{-d,\varepsilon} = \exp[-\hat{D}(\omega,\varepsilon h)]$ and the dispersive walk-off is not included.
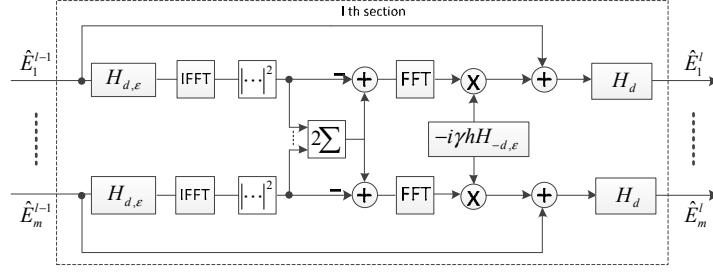
Fig. 1. Block diagram for the implementation of the lth section using the develop perturbation technique.

3. Analysis of computational complexity

It is significant to investigate the computation requirements for APT and C-DBP where conventional symmetric SSM is employed. For simplicity only the number of complex multiplications will be considered, neglecting the number of additions. Furthermore, considerations regarding the numeric representation (fixed point/floating point) will be ignored. By following the schematic diagram in Fig. 1, the total number of required multiplications per sample per channel for each method is given by:

$$Nmul_{DPT} = \frac{L}{h_{DPT}}[2(s+p)\log_2(s+p)+3(s+p)+s]/s, \qquad (11)$$

$$Nmul_{C-DBP} = \frac{L}{h_{C-DBP}}[2(s+p)\log_2(s+p)+2(s+p)+8s]/s, \qquad (12)$$

where S is the number of samples per channel, L is the total transmission distance, h is the corresponding step size and p is the overhead samples for each filter operation when the filter implementation in the frequency domain is done by the overlap-and-add method and can be obtained by [24]: $p = 2\pi|\beta_2|BhR$, where R is sampling rate and B is bandwidth. The number of multiplications for each operation involved in backward propagation is calculated as follows. The filter requires $2(s+p)\log_2(s+p)+(s+p)$ multiplications; intensity operator requires s multiplications; exponential operator (4th order Taylor expansion) requires $6s$ multiplications and the further details of the approach to calculate the number of multiplication can be found in [25]. As s is much larger than p normally ($s >> p$), when the step size of both methods is assumed to equal span length, it is obvious that about $6N$ more multiplications per sample per channel will be required for C-DBP than APT.

4. Numerical simulation results and discussion

Numerical simulations using MATLAB were conducted to investigate the benefit of the advanced perturbation technique compared with C-DBP where conventional symmetric SSM is employed. An 8 × 80 *Gbit/s* channel QPSK WDM system distributed around 1550 *nm* with channel spacing of 50 *GHz* has been simulated as shown in Fig. 2. The optical link consists of 20 spans of single mode fiber (SMF) with a length of 80 *km* per span, a dispersion parameter of *D = 16.5 ps/nm/km* and a dispersion slope of *Ds = 0.04 ps/nm2/km*. The attenuation of the fibre is 0.2 *dB/km* and the nonlinear coefficient is *γ = 1.46 (W.km)$^{-1}$*. Fibre loss is compensated per span using an EDFA, which will introduce ASE noise with the average power $I_{ASE} = N_{sp}\hbar\omega_0(G-1)B$ where G is the amplifier gain, $\hbar$ is Plank's constant, B is the bandwidth, and N_{sp} is the spontaneous emission factor. 2^{10} pseudo-random bit sequences (PRBS) with non-return-to-zero QPSK modulation were transmitted through the system. The

forward propagation is modeled by solving the exact NLSE using symmetric SSM [21]. To provide an accurate result, the step-size is sufficiently short to keep the nonlinear phase-shift much less than 0.05 degrees. Local oscillators are used for reconstruction of each WDM channel and assumed to have zero linewidth. After transmission and coherent detection, the received signal is filtered using a 0.75 times bit rate bandwidth sixth order Bessel band-pass filter. Then each channel is sampled at 2 *samples/symbol* and backward propagated using Eq. (1). After backward propagation, demultiplexing is performed. Then the signal in each channel is re-sampled to one sample per symbol and phase estimation is performed to recover the data.
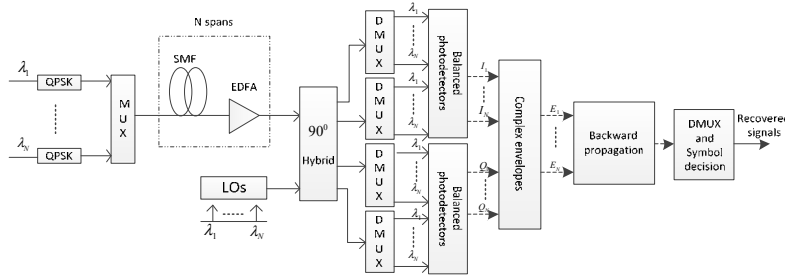

Fig. 2. Scheme of the WDM transmission system with coherent receiver.

Figure 3 shows the Q-factors as functions of step size (SS) and a long fiber transmission distance for C-DBP, APT and TPT implementations with launch power at −2 *dBm*, which is optimum launch power for APT when $\gamma = 1.46 \ (W.km)^{-1}$. Agreeing with theoretical analysis in section 2, the Q-factor of TPT declines very fast with raising step size as shown in Fig. 3(a). Meanwhile, as shown in Fig. 3(b), when step size of both TPT and APT are set to 8 *km* in a long fiber transmission distance, the Q-factor of TPT is far less than APT and even less than APT with step size 80 *km*, which means TPT is unsuitable for application to DBP. Figure 3(a) shows that since the performance of C-DBP will be improved with a shorter step size, the Q-factors of both C-DBP and APT are almost the same when step size is sufficiently short (<20 *km*). But, with the step size increasing, the Q-factor of C-DBP decays faster than APT. When step size is greater than 20 *km*, APT performs significantly better than C-DBP. Particularly, APT produced an improvement about 0.85 *dB* than C-DBP for one step per span, which is a typical value of step size in practice. It indicates that APT will reduce the number of steps for similar performance. Therefore, the majority of the benefit of APT is obtained with larger step. Figure 3(b) shows an efficient compensation of fiber inter-nonlinear and dispersion impairments using ATP. Comparing to chromatic dispersion (CD) compensation, a large benefit about 6.7 *dB* for SS = 8 *km* and 5.2 dB for SS = 80 *km* with 1600 *km* transmission distance is provided by APT from inter-nonlinear compensation.
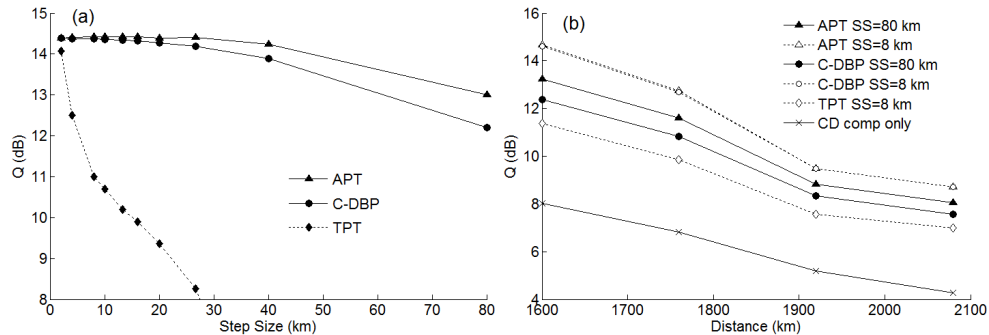

Fig. 3. (a) Q-factors as a function of step size for APT, C-DBP and TPT, (b) Q-factors versus a long fiber transmission distance for APT, C-DBP, TPT and only chromatic dispersion compensation with different step size.

To show the benefit of APT in a transmission system, the relationship between Q-factor and launch power with various fiber nonlinear coefficients γ for linear equalization and nonlinear equalization using APT and C-DBP is the most interesting issue, which is shown in Fig. 4. The step sizes of both methods are located at one step per span. At low powers, as the nonlinear effects are weak, the system behaves as a linear system. Due to a good linearity compensation for both of APT and C-DBP, no improvement is produced by nonlinearity compensation and for $γ = 0$ $(W.km)^{-1}$ both methods give the same performance.

Figure 4 show that APT gave better performance than C-DBP. For both methods there was <1 *dB* penalty compared to the linear case ($γ = 0$) for launch powers lower than −6 *dBm*. The penalty increases rapidly at higher launch powers with the onset of the increase being dependent on the value of γ and the method used. The optimum launch power was approximately 1 *dBm* higher for APT than C-DBP and that the performance of APT was approximately 0.5-0.7 *dB* higher than C-DBP at their respective optimum powers. For the same launch power the benefit of APT increases with launch power and that the nonlinear tolerance of APT is significantly better than C-DBP for launch power greater than −5 *dBm* for $γ = 3.5$ *(W.km)*$^{-1}$ and −2 *dBm* for $γ = 1.46$ *(W.km)*$^{-1}$, especially, APT produced a benefit about 2.4 *dB* at 3 *dBm* for $γ = 1.46$ *(W.km)*$^{-1}$ and 2.7 *dB* at −1 *dBm* for $γ = 3.5$ *(W.km)*$^{-1}$. This suggests that APT is a more accurate method for nonlinearity compensation than C-DBP, especially for higher launch power. The nonlinear coefficient *3.5 (W.km)*$^{-1}$ does not represent any practical interest.
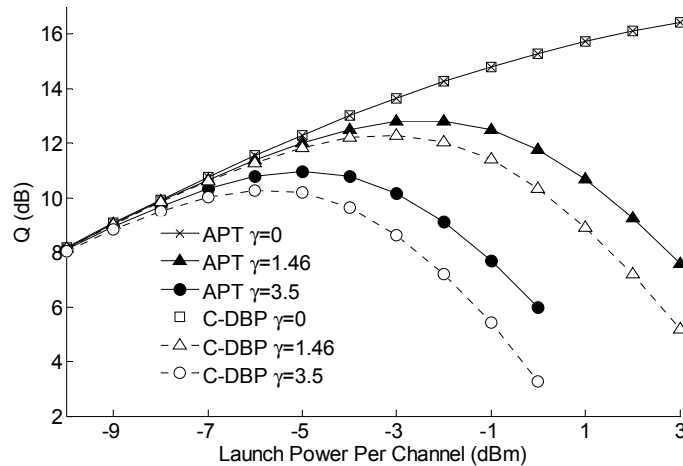

Fig. 4. Q-factors versus launch power per channel for both methods for γ = 1.46 and 3.5 (W.km)$^{-1}$

Due to the significant influence of oversampling rate for computational load, it is necessary to display the performance of APT and C-DBP with different oversampling factors, as shown in Fig. 5. One step per span is used as the step size in this comparison. The results in Fig. 5(a) show the Q factor for APT and C-DBP for oversampling factors of 2 and 4. By comparing the Q value at the optimal launch powers in Fig. 5(a) it is clear that the oversampling factor can be reduced by using APT with only a small Q penalty. When launch power is −10 dBm, there is about 3.2 dB benefit of oversampling factor of 4 than 2. This is because a higher oversampling rate provides each symbol carrying more information to get a better distinction between signal and noise levels in backward propagation. Therefore larger Q-factors were obtained with a higher oversampling factor for both methods. The maximum Q value for C-DBP with an oversampling factor of 4 was 13.8dB at a launch power of −4dBm which is only 0.3dB higher than the 13.5dB optimal Q value of APT with an oversampling factor of 2 at −2dBm launch power. This factor of two reduction in oversampling factor

would significantly relax the specification of analogue to digital converter hardware in the receiver as well as being more computationally efficient.

Further analysis of these results as shown in Fig. 5(b) indicates that when the same oversampling factor is used for both methods and the launch power is low (below −4 *dBm*) there is less than 0.5 *dB* difference in the Q factors. This is as expected as the transmission at these launch powers is largely unaffected by nonlinear impairments. However as launch power is increased and nonlinear impairments increase, APT performs better than C-DBP. The performance difference is similar for both oversampling factors used and the results show that the difference in Q factors increases approximately linearly with a slope of ~0.4 *dB/dBm* over the range of input powers from −2 *dBm* to 3 *dBm*.
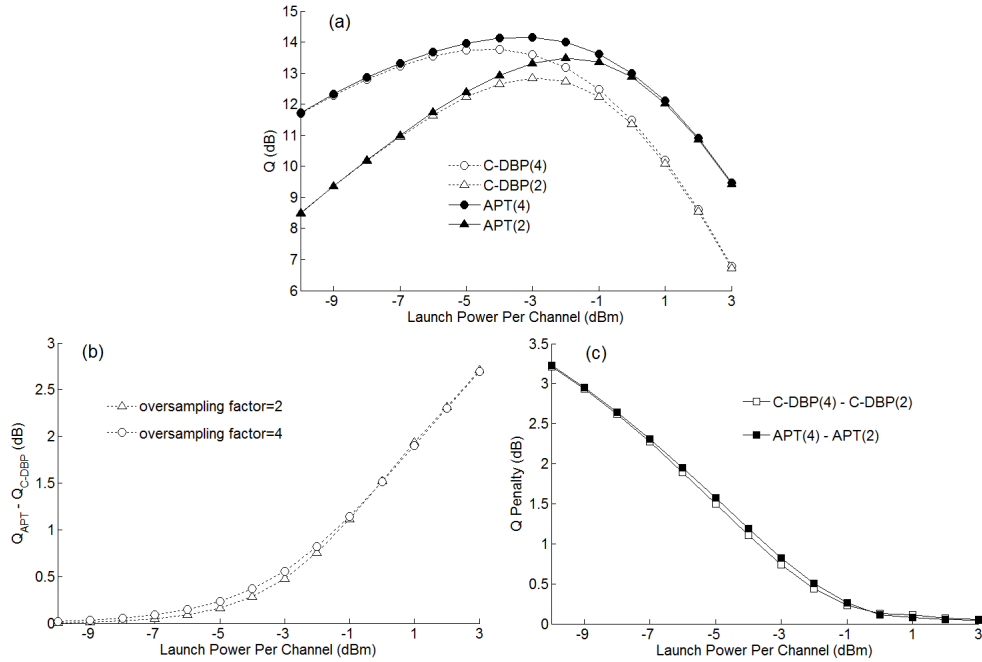

Fig. 5. (a) Q-factors versus launch power per channel for APT and C-DBP with oversampling factors of 2 and 4, (b) Q penalty for reduced oversampling factor for APT and C-DBP and (c) Q factor difference between APT and C-DBP for oversampling factors of 2 and 4.

Figure 5(c) shows the penalty associated with reduction of the oversampling factor from 4 to 2 for each method. It is clear that both methods show very similar performance: since the power of ASE noise doesn't change with channel power, when launch power is low (<-2 *dBm*), as the explanation mentioned-above, larger Q-factors were obtained with a higher oversampling factor for both methods. As the launch power was increased, the advantage of using the higher oversampling factor decreased approximately linearly at a rate of ~0.1 *dB/dBm* up to a launch power of −2 *dBm*. For launch power greater than 0 *dBm*, the oversampling factor had little influence due to the higher OSNR, which agrees with previous experimental results [6,19]. For this high power nonlinear regime the results show a clear advantage for APT over C-DBP: for a launch power of 3 *dBm*, APT gives an improvement of 2.7 *dB* in Q-factor compared to C-DBP. Due to the benefits of APT discussed previously, reductions in both step size and sampling rate can be obtained when both methods perform at the same accuracy, launch power is higher than 0 *dBm* and the nonlinear coefficient is larger than 1.46 *(W.km)⁻¹*, and meanwhile, combining a reduction in multiplications per sample per channel per section by a factor of around six which is discussed in section 2, we estimate that there is a reduction in computational complexity by a factor of around seven.

Further studies about the performance of APT and C-DBP with different number of WDM channels have been done at −2 dBm. Step sizes of both methods are located at one step per span. The results indicate that APT give better performance than C-DBP with various number of WDM channels and the benefit of APT increases with number of WDM channels, especially, APT produced a benefit about 1.2 dB for 8 channels and 2.5 dB for 24 channels.

5. Conclusion

We propose an advanced perturbation technique (APT) for digital backward propagation in WDM systems using the coupled nonlinear Schrodinger equations for the compensation of inter-channel nonlinearities. An analytical expression of the output after backward propagation is obtained initially, which could be extended to include the inter-channel walk-off effect. Computer simulations have been carried out comparing the proposed technique with conventional digital back-propagation (C-DBP) for various simulation parameters. Our research indicates that this advanced perturbation technique can reduce computational load significantly and is more accurate than C-DBP for nonlinearity compensation when launch power is higher than −2 dBm and step size is larger than 20 km, which will allow larger step size for equivalent performance. Meanwhile, APT requires a lower sampling rate when launch power is higher than −2 dBm. Furthermore, our technique also has the potential to ease requirements of receiver hardware components which would be used in a practical implementation. We estimate a reduction by a factor of around seven in computational load with respect to the C-DBP technique. This computational efficiency improvement and potential reduced hardware performance requirements of the advanced perturbation technique reported here a step towards making nonlinear compensation based on back propagation implementable in real-time.